

Non-contact monitoring during laser surgery by measuring the incision depth with air-coupled transducers

Francisco Javier Oyaga Landa^{1,2} and Xosé Luís Deán-Ben¹ and Francisco Montero de Espinosa³ and Daniel Razansky^{1,2,*}

¹Institute for Biological and Medical Imaging (IBMI), Helmholtz Zentrum München, Neuherberg, Germany

²School of Medicine, Technische Universität München (TUM), Munich, Germany

³CSIC, Institute of Physics and Communication Technologies, Madrid, Spain

*Corresponding author: dr@tum.de

ABSTRACT

Lack of haptic feedback during laser surgery hampers controlling the incision depth, leading to a high risk of undesired tissue damage. Here we present a new feedback sensing method that accomplishes non-contact real-time monitoring of laser ablation procedures by detecting shock waves emanating from the ablation spot with air-coupled transducers. Experiments in soft and hard tissue samples attained high reproducibility in real-time depth estimation of the laser-induced cuts. The advantages derived from the non-contact nature of the suggested monitoring approach are expected to greatly promote the general applicability of laser-based surgeries.

Keywords: Remote sensing and sensors; Ablation of tissue; Process monitoring and control; Photoacoustics; Photoacoustic imaging

1. INTRODUCTION

Laser surgery is an advantageous alternative to scalpel-based procedures, which are often afflicted with excessive mechanical traumatization and bacterial contamination. Laser-based incisions offer minimally-invasive intervention with less collateral damage, more efficient hemo- and bacterio-stasis, less postoperative pain and swelling.¹ These advantages have inspired the application of pulsed laser surgery in a wide range of clinical procedures involving cutting soft and connective tissues e.g. in dermatology, ophthalmology or oncology.¹⁻⁵ Yet, the lack of haptic feedback and real-time control over the lesion profile are the major drawbacks of laser-based surgical procedures, severely limiting the range of their potential applications.⁴⁻⁸

Pulsed laser ablation consists in vaporization and ejection of tissues, leading to generation of laser-induced shock waves at the incision spot. This ablation mechanism is already exploited by an ample spectrum of laser-tissue applications.⁹⁻¹² For example, it has been shown that efficient laser osteotomy can be performed at laser fluence levels of around 160 J/cm².¹³ Recently, it was demonstrated that acoustic detection of shock waves can be used as a feedback mechanism to monitor the incision depth during laser ablation. By using a matrix array of ultrasound detection elements, the feasibility of three-dimensional (3D) localization of the incision profile was showcased in ex-vivo samples.¹⁴ However, the need of an acoustic matching medium (typically water or ultrasound gel) between the ablated tissue and the feedback detector may still hamper the applicability of this approach in a real clinical setting.

It has been previously shown that the non-contact detection of pressure (ultrasound) waves from remote locations is possible by means of air-coupled transducers,¹⁵ which are specifically designed to reduce the enormous acoustic mismatch between air and ultrasound sensing elements. Efficient coupling to the air medium can be performed with micro-membrane capacitance transducers¹⁶ or with piezoelectric sensors coupled with microporous layers, with the latest approach more convenient for frequencies above 1 MHz.¹⁷ Air-coupled transducers have recently been shown to provide sufficient sensitivity in non-contact optoacoustic (OA) imaging using laser fluence levels below 20 mJ/cm².¹⁷ It is therefore expected they are ideally suitable for efficient detection of shock waves generated during laser ablation procedures, where the fluence levels may exceed 10 J/cm² for some applications.¹⁸ In this work, we describe a method based on the feasibility of using air-coupled transducers to monitor the incision depth in laser cutting from the measured time-of-flight of the generated pressure waves.

This approach can potentially be applicable as a method in surgical procedures, where liquid acoustic coupling may constitute a major disadvantage.¹⁹

2. MATERIALS AND METHODS

A lay-out of the experimental setup is shown in Figure 1a. Laser ablation was performed with a frequency-doubled Q-switched Nd:YAG laser (Spectra Physics, Santa Clara, CA) operating at 532 nm with a pulse duration of approximately 7 ns. In order to create ablation, we used per-pulse energies above 40 mJ and a pulse repetition frequency of 15 Hz. The laser beam was focused using a lens with 150 mm focal distance (Thorlabs, Newton, NJ). In all experiments, the focal point was located approximately 3 mm under the tissue surface. We characterized the ablation beam size as a function of distance using a camera-based SP620U beam profiler (Spiricon Ophir Photonics, North Logan, UT). The beam diameter shrinks down to 30 μm at the focus, inducing fluence levels up to 5 KJ/cm^2 (Fig. 1b). Under these conditions, the laser beam was able to perform deep incisions attaining relatively low collateral thermal damage. Laser ablation was performed in both soft and hard (bone) tissue. Specifically, three different types of tissue were ablated, including liver cheese (German: Leberkäse), chicken breast and chicken bone. The tissue samples were carefully prepared before the experiment. While leberkäse samples are considered to be relatively heterogeneous, fat and connective tissue were removed from chicken breast and bone tissues, resulting in more homogeneous samples.

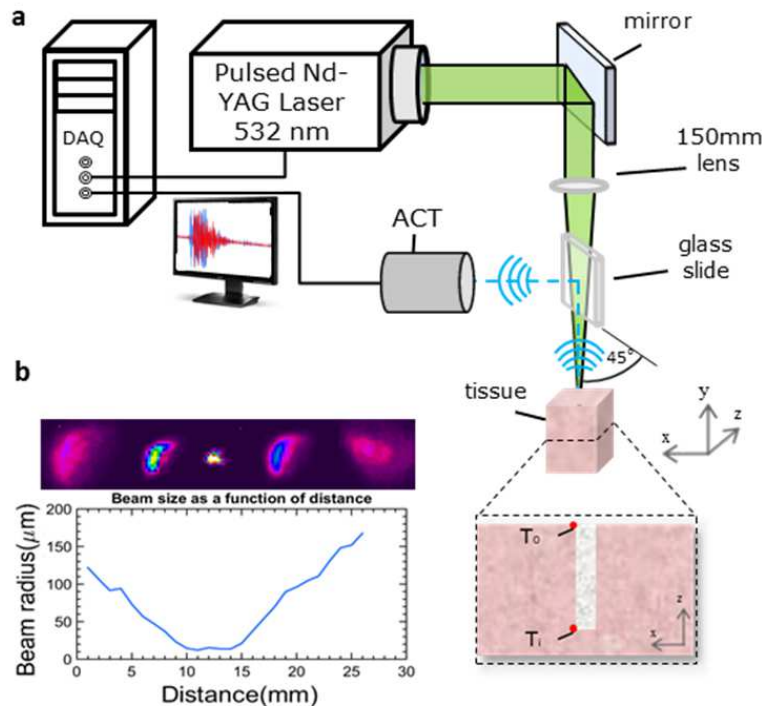


Figure 1. (a) Lay-out of the experimental setup. ACT (air-coupled transducer), DAQ (data acquisition), Nd:YAG (neodymium-doped yttrium aluminium garnet). The glass slide (1.1 mm thickness) is positioned at 45° relative to the shockwaves propagation direction, so that the acoustic waves are reflected at 90° . (b) Ablation beam characterization in the vicinity of the focal region. Typical beam shapes are shown in the inset. The depth of focus is approximately 5 mm. Cross-section of the perforated tissue showing the location of the two points used to calculate the time of flight difference.

Shockwaves emitted from the ablation spot were detected with a self-developed unfocused air-coupled piezo-

electric transducer with a central frequency of 0.8 MHz and -6dB bandwidth of 0.4 MHz.²⁰ The transducer is based on a flat 1-3 piezocomposite with a 20 mm diameter active area. It was positioned at an acoustic travel distance of 50 mm from the tissue surface using a glass slide oriented at 45° so that the light beam can propagate without changing its direction while the acoustic waves are reflected at 90° (Fig. 1). The pressure signals collected by the transducer were amplified by 30 dB and digitized at 10 megasamples per second with 12-bit vertical resolution by means of a PCI Express acquisition card (Model ATS9351, AlazarTech, Pointe-Claire, QC, Canada) triggered with the Q-switch output of the laser.

The time of arrival of the measured shockwaves was estimated as the instant for which the pressure signal level exceeds a defined threshold. The threshold was set to 16% of the maximum value for the entire signal sequence. It was further assumed that the ablation spot is always located at the bottom of the cut so that it deepens as the incision progresses with the consequent time of arrival delay of the shockwaves to the transducer surface. The time of flight difference (*TOFD*) of the generated shockwaves within the open cut is then estimated as the difference in the time of arrival T_i for each detected shock wave with respect to an average time of arrival T_0 for the signals generated by the first 20 laser pulses. If the speed of sound within the incision c_i is known, one could then provide an estimate on the incision depth d according to

$$d = c_i \cdot TOFD. \quad (1)$$

3. RESULTS

For the experiments, we used 40 Leberkäse samples, 30 samples of chicken breast and 20 samples of chicken bone. The incision depths ranged from 1 to 4 mm for soft tissue samples (Leberkäse and chicken breast) and from 1 to 8 mm for the osseous tissues. Figure 2a-c shows examples of signals recorded by the air-coupled transducer for the 3 different tissue types. The recorded waveforms are increasingly delayed as the incision progresses, which indicates deepening of the lesion. Examples of the measured time of arrival of the shockwaves as a function of time are further shown in Figures 2d-f. It is expected that the shockwaves generated by the laser pulse propagate at supersonic speeds in the immediate vicinity of the ablated spot but rapidly slow down to the speed of sound for normal (linear) wave propagation.²¹

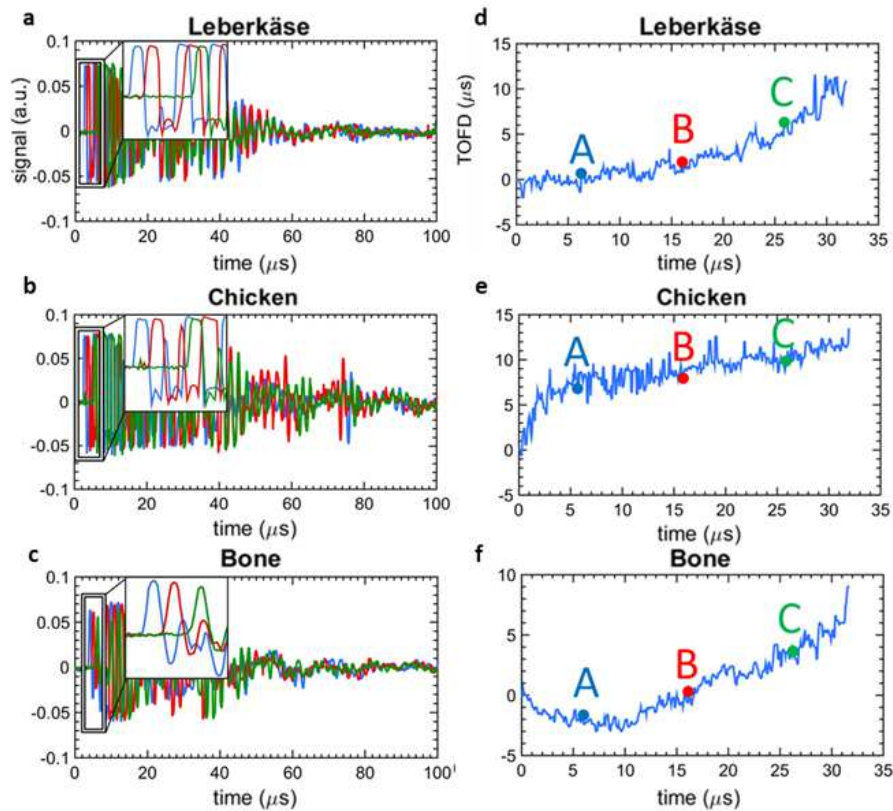


Figure 2. Illustration of the method used to measure SOS for different tissue types. Examples of the recorded signals for Leberkäse (a), chicken (b) and bone (c). Each color corresponds to 3 different instants, namely, 6s (blue), 16s (red) and 26s (green) after the ablation start. Evolution of the corresponding *TOFD* is in (d), (e) and (f).

Note that variations in the *TOFD* differ between the tissues. For instance, a 2 s delay of the time of arrival was observed for leberkäse (Fig 2d) following 300 laser shots, whereas the corresponding delay for the chicken breast (Fig. 2e) and bone (Fig. 2f) was 5.5 s and 1 s, respectively. One may note that the time of arrival has decreased during the first 150 laser pulses for the bone tissue, which can be attributed to the thermoelastic expansion of the surface as the laser penetrates into the lower layers of the compact bone. The time of arrival consistently exhibits an unsteady behavior in the starting phase of the ablation. The recorded time-resolved signals are characterized by lengthy oscillations due to generation of optoacoustic signals due to residual light absorption in previously generated tissue debris within the crater. Some abrupt variations in the time of arrival can be also attributed to ablation events occurring in air before the light pulses reach the tissue. The values of the speed of sound inside the incision were subsequently estimated by considering the actual (final) incision depth d_f measured in post-ablated tissue slices and the average time of flight difference recorded for the last 20 laser pulses $TOFD_f$ via

$$c_i = d_f / TOFD_f. \quad (2)$$

The calculated values of c_i are shown in Figure 3 as a function of the measured final incision depth. One may see that, for soft tissue samples, the average estimated c_i increases versus incision depth (Figs. 3a and 3b). Specifically, c_i reaches average values of 750 m/s and 570 m/s for 3-4 mm cuts in the leberkäse and chicken

breast specimen, respectively. For shallow incisions, the average c_i values remained close to the speed of sound in air (343 m/s for dry air at 20°C). This may indicate that deeper cuts in soft tissue samples have been filled up with material expelled by the ablation events, so that the shockwaves propagate through a mixed air-tissue medium. Conversely, the average value of c_i better matches the speed of sound in air for bone samples, even for considerably deeper cuts (Fig. 3c). This appears to indicate that the extracted volume is mainly filled with air during the ablation of bones. Finally, by substituting the c_i values according to the linear fits in Figs. 3a-c and the measured TOFD values from Fig. 2 into Eq. 1, one may obtain real-time estimates for the incision depth for the three experiments presented in Fig. 2, as shown in Figs. 3d-f.

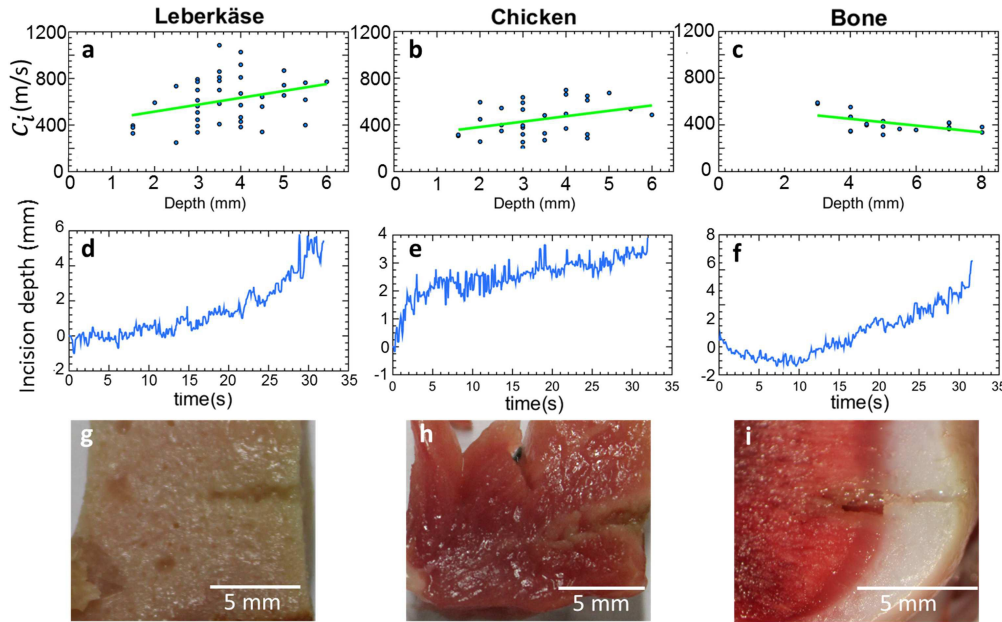


Figure 3. (a)-(c) Distribution of the estimated speed of sound within the incision based on measurements performed on sliced specimen. Green lines correspond to the linear fit through the scattered data. Examples of real-time incision depth estimations for each tissue type are presented in (d)-(f). The actual photographs of the sliced samples are shown in (d), (e) and (f) respectively.

4. DISCUSSION

The presented results demonstrate the basic feasibility of attaining real-time feedback on the laser-induced incision depth by means of non-contact detection of the generated shock waves with air-coupled transducers. Several clinical applications may greatly benefit from this newly discovered approach. In melanin pigmentation treatments, maxillofacial surgery, precancerous lesion or benign tumor removal, the performance of laser-based surgery procedures is often hindered by the lack of online depth monitoring. According to the presented results, our method is anticipated to provide accurate estimates on the incision depth in bones, making it ideally suited for accurate monitoring of lesion depth in laser osteotomy. Accordingly, the higher variability of speed of sound inside soft tissue incisions is expected to introduce corresponding uncertainties into the incision depth estimates. However, this variability remains low for incision depths below 1-2mm where the method is expected to provide accurate estimates. It is further expected that more accurate selection and calibration of the ablation parameters for the different tissue types (laser energy, focal distance, optical fluence at the surface) may further enhance

the performance of the method. In conclusion, we presented a new method for monitoring of laser ablation procedures, which accomplishes real-time tracking of the incision depth by detection of shock waves emanating from the ablation spot with air-coupled transducers. The advantages derived from the non-contact nature of the suggested monitoring approach are expected to greatly promote the general applicability of laser-based surgeries.

ACKNOWLEDGMENTS

Deutsche Forschungsgemeinschaft (DFG) (RA1848/5-1); Comisin Interministerial de Ciencia y Tecnologa (CI-CYT) (DPI201346915-C2-1-R).

REFERENCES

1. J. T. J. Walsh and T. F. Deutsch *Appl. Phys.* **B 52**, p. 217, 1991.
2. R. O. Esenaliev, A. A. Oraevsky, V. S. Letokhov, A. A. Karabutov, and T. V. Malinsky *Lasers Surg. Med.* **13**, p. 470, 1993.
3. T. Juhasz, X. H. Hu, L. Turi, and Z. Bor *Lasers Surg. Med.* **15**, p. 91, 1994.
4. F. W. Neukman and F. Stelzle *Phys. Procedia* **5**, p. 91, 2010.
5. G. K. Eyrich *Med. Laser Appl.* **20**, p. 25, 2005.
6. J. M. White, H. E. Goodis, and C. L. Rose *Lasers Surg. Med.* **11**, p. 455, 1991.
7. A. Tuchmann, P. Bauer, H. Plenk, and O. Braun *Res. Exp. Med.* **186**, p. 375, 1986.
8. A. Vogel and V. Venugopalan *Chem. Rev.* **103**, p. 577, 2003.
9. F. Stelzle, A. Zam, W. Adler, K. Tangermann-Gerk, A. Douplik, E. Nkenke, and M. Schmidt *J. Transl. Med.* **9**, p. 20, 2011.
10. D. C. Jeong, P. S. Tsai, and D. Kleinfeld *Curr. Opin. Neurobiol.* **22**, p. 24, 2012.
11. A. M. R. B. M. M. B. M. Kim, M. D. Feit and L. B. D. Silva *Appl. Surf. Sci.* **857**, pp. 127–129, 1998.
12. K. Nahen and A. Vogel *Lasers Surg. Med.* **25**, p. 69, 1999.
13. S. Stbinger, B. von Rechenberg, H. Zeilhofer, R. Sader, and C. Landes *Lasers Surg. Med.* **39**, p. 583, 2007.
14. L. Fichera, C. Pacchierotti, E. Olivieri, D. Prattichizzo, and L. S. Mattos *IEEE Haptics Symposium*, pp. 59–64, 2016.
15. M. J. Garcia-Hernandez, J. A. Chavez, Y. Yaez, H. B. Kichou, J. L. Prego-Borges, J. Salazar, A. Turo, and F. M. de Espinosa *IEEE Int. Ultrason. Symp.* **2**, p. 1282, 2004.
16. S. T. Hansen, F. L. Degertekin, and B. T. Khuri-Yakub *Proc. SPIE* **3586**, p. 310, 1999.
17. T. E. G. Alvarez-Arenas *Sensors* **13**, p. 5996, 2013.
18. X. L. Den-Ben, G. A. Pang, F. M. de Espinosa, and D. Razansky *Appl. Phys. Lett.* **107**, p. 051105, 2015.
19. F. J. O. Landa, X. L. Deán-Ben, F. M. de Espinosa, and D. Razansky *Opt. Lett.* **41**, pp. 2704–2707, 2016.
20. E. Bay, A. Douplik, and D. Razansky *Lasers Med. Sci.* **29**, p. 1029, 2014.
21. T. E. Gomez and F. M. de Espinosa *IEEE Ultrason. Symp.* **2**, p. 1069, 2000.